CRIME MODELLING WITH LÉVY FLIGHTS AND THE STABILITY OF HOT-SPOT PATTERNS

JONAH BRESLAU, TUM CHATURAPRUEK, THEODORE KOLOKOLNIKOV,
SCOTT MCCALLA, DANIEL YAZDI

ABSTRACT. Working off of the pioneering crime modeling paper of Short *et al.* (2008), we alter the movement patterns of the criminal agents to follow biased Lévy Flights rather than biased Brownian motion in the original discrete model. This, in turn, leads in the continuum limit to the use of the fractional Laplacian or Riesz Derivative, Δ^s, to represent the diffusion of the criminals, which converges to the traditional Laplacian when $s = 1$, where s is the Lévy Flight non-locality parameter. We also find a novel bifurcation for the linear stability near the spatially homogeneous equilibrium in the Lévy Flight non-locality parameter, s. Finally, we estimate the profile of the hotspots.

Keywords: fractional Laplacian, super-diffusion, hot-spots, Lévy flights, crime modeling, bifurcations and instability

1. INTRODUCTION

Crime is unfortunately a common component of the society we live in. Furthermore, it is not uniformly distributed, with certain neighborhoods containing high levels of criminal activity in comparison to others. The regions of space containing elevated criminal activity in a short period of time are known as hot-spots. In their seminal paper, Short *et al.* pioneered the movement for applying mathematical models for understanding the dynamics of criminal activity. Specifically, they focused on residential burglaries due to the simplicity of accounting for moving offenders and stationary victims [13].

The model incorporates the assumptions of repeat/near repeats events and the broken window theory, which are supported by empirical evidence. Repeat/near repeat events reason there is a high likelihood of being robbed a second time shortly after a home or a neighbor's home is robbed for the first time. This increased probability decays through time and is due to factors such as the criminal's familiarity/comfort with the neighborhood and knowledge of other goods to be stolen [11]. The broken window theory takes into account the diffusive nature of crime. Neighborhoods with high crime exude a sense of lawlessness, and a notion of crime tolerance. As a result, homes in such neighborhoods can become more desirable targets for burglars.

Another critical assumption of the original model is that criminals travel through space with a biased Brownian motion. In the discrete model, this amounts to criminals moving to adjacent homes, and in the continuous case, moving with biased regular diffusion. With this motion, robbers have limited knowledge that is restricted to the homes directly adjacent to them. In addition, it assumes this is a natural mode of human mobility. However, this is not necessarily a safe assumption. It has been shown that humans and other animals follow a Lévy flight style of movement [10, 3]. Instead of moving to adjacent neighbors, Lévy flght allows for longer jumps to be made with the probability dictated by a power law distribution. The non-local fractal nature of this motion allows criminals to have extended knowledge of their surroundings, and allows them to more efficiently examine the space for potential homes to rob.

For this project, we have adjusted the Short *et al.* model to have criminals move in a non-local manner. With this new condition, we constructed an agent based model for residential burglaries, and derived a series of partial differential equations representing the system. Specifically, the new model contains the fractional Laplacian, a non-local extension of the normal Laplacian, which allows for the super-diffusion of criminals. Linear stability analysis was performed to identify the conditions rendering hot-spot formation. This includes an analysis of how transitioning from Brownian motion to Lévy flight can alter hot-spot formation. Furthermore, we simulated our mathematical findings using spectral methods and verified our results with numerical simulations across the parameter space. We conclude our study with an exploration of the analytic solution describing hot-spot morphology under Lévy flight motion. We hope our findings provide a more realistic and accurate representation for the dynamics of residential burglaries.

2. Modeling Fractional Diffusion

2.1. Original Short *et al.* Model.

2.1.1. *Discrete Model.* Short *et al.* first start off by creating a discrete, agent-based model [13]. They begin by defining the attractiveness of each location s at time t, $A_s(t)$, which is then partitioned into a static background component A_0 and a dynamic component $B_s(t)$:

$$A_s(t) \equiv A_s^0 + B_s(t). \tag{2.1}$$

The robbers' movements are biased towards areas of high attractiveness. Their probability of movement from sites to the neighboring site n is

$$q_{s\to n}(t) = \frac{A_n(t)}{\sum_{s'\sim s} A_{s'}(t)}, \tag{2.2}$$

where $s' \sim s$ signifies all the gridpoints s' adjacent to s. The probability that a given burlglar robs location s betwen times t and $t+\delta t$ is

$$p_s(t) = 1 - e^{-A_s(t)\delta t}. \tag{2.3}$$

Robbers are removed from the grid after they rob a home, to model returning home with the goods. Let $N_s(t+\delta t)$ be the number of robbers at s at time $t+\delta t$. Then

$$N_s(t+\delta t) = \sum_{s'\sim s} N_{s'}(t)(1-p_{s'}(t))\cdot q_{s'\to s} + \Gamma, \tag{2.4}$$

which is derived from the number of criminals from neighboring cells who do not commit crime and move to s following the biased transition probability given above plus a constant replenishment rate Γ.

The formula for the dynamic attractiveness is

$$B_s(t+\delta t) = [B_s(t) + \frac{nl^2}{z}\Delta B_s(t)](1-\delta t) + \theta E_s(t), \tag{2.5}$$

where Δ is the discrete Laplacian operator

$$\Delta B_s(t) = \left(\sum_{s`\sim s} B_{s'}(t) - zB_s(t)\right)/l^2. \tag{2.6}$$

2.1.2. *Continuous Model.* To derive the continuum model, let $\rho = N/l^2$ and let δt and l go to zero with the constraint $l^2/\delta t = D$ and $\theta\delta t = \varepsilon$ to get

$$\frac{\partial B}{\partial t} = \frac{\eta D}{z}\nabla^2 B - \omega B + \varepsilon D\rho A. \tag{2.7}$$

The derivation of the continuum limit of $N(t)$ is more complicated.
For one dimension, our goal is to get

$$N_t - \Gamma + \frac{2D}{z}\left(\frac{N}{A}A_x\right)_x = \frac{D}{z}N_{xx} - NA. \tag{2.8}$$

We note

$$1 - p_s^t \sim 1 - A\delta t, \tag{2.9}$$

and that

$$\frac{1}{\sum_{s''\sim s'} A_{s''}(t)} = \frac{1}{zA_{s'} + l^2\Delta A_{s'}} \sim \frac{1}{zA_{s'}}\left(1 - \frac{l^2\Delta A_{s'}}{zA_{s'}}\right) \tag{2.10}$$

Expanding the discrete mode (2.4), we have

$$N_t - \Gamma = \frac{A_s}{\delta t}\sum_{s'\sim s}\left[\left(\frac{N_{s'}}{zA_{s'}}\right) - \left(\frac{N_s}{zA_s}\right) - \frac{N_{s'}\delta t}{z} - \frac{N_{s'}}{(zA_s)^2}D\delta t\Delta A_{s'}\right] \tag{2.11}$$

$$= \frac{AD}{z}\left(\frac{N}{A}\right)_{xx} - NA - \lim_{l\to 0} DA_s\left(\sum_{s'\sim s}\frac{N_{s'}}{(zA_s)^2}\Delta A_{s'}\right) \tag{2.12}$$

$$= -\frac{2D}{z}\left(\frac{NA_x}{A}\right)_x + \frac{D}{z}N_{xx} - NA. \tag{2.13}$$

Let $\rho = N/l^2$ and fix $\Gamma/l^2 = \gamma$ and we get

$$\frac{\partial\rho}{\partial t} = \frac{D}{z}\nabla\cdot\left[\nabla\rho - \frac{2\rho}{A}\nabla A\right] - \rho A + \gamma, \tag{2.14}$$

and these two equations are in the general form of a reaction-diffusion system. Note also that this can be written:

$$\frac{\partial\rho}{\partial t} = \frac{D}{z}\left[A\Delta\frac{\rho}{A} - \frac{\rho}{A}\Delta A\right] - \rho A + \gamma,$$

One interesting observation is that if we integrate the steady-state version equation of the second PDE, and assuming either a Neumann or a periodic boundary condition, the result is that the spatially averaged criminal density is constant at γ [13].

Similarly, the spatially homogeneous attractiveness value is also constant at $\bar{B} = \frac{\varepsilon D\gamma}{\omega}$. Now, here is a dimensionless version of the two governing PDEs

$$B_t = \eta B_{xx} - B + \rho A \tag{2.15a}$$

$$\rho_t = (\rho_x - 2\rho\frac{A_x}{A})_x - \rho A + \overline{B} \tag{2.15b}$$

2.2. **Non-local Walking Criminal Model.** Given the evidence cited above, a Lévy flight model of human mobility may better represent the movement of criminals than the current Brownian motion-like assumptions of Short *et al.* First, for simplicity, we look at the discrete model on the real line on which the grid size is l. Point 1, for example, corresponds to l in the actual real line number. We define the relative weight of a criminal moving from point i to point s, where $i \neq s$, as

$$w_{i\to s} = \frac{A_s}{d(s,i)^\mu}, \tag{2.16}$$

where μ is a constant in the interval $(1, 3)$, and $d(s, i) = l|s - i|$. The range for μ in a 1D model and a 2D model will be different. Now we normalize that relative weight to get the probability of a criminal moving from point i to point s, where $i \neq s$,

$$q_{i\to s} = \frac{w_{i\to s}}{\sum_{j\in\mathbb{Z}, j\neq i} w_{i\to j}}. \tag{2.17}$$

Thus, our criminals follow a kind of biased Lévy Flight. Considering the denominator, we can write it in the following manner (the reason for doing this will be apparent when we take the limit $l \to 0$)

$$\begin{aligned}\sum_{j\in\mathbb{Z},j\neq i} w_{i\to j} &= \sum_{j\in\mathbb{Z},j\neq i} \frac{A_j}{d(j,i)^\mu} \\ &= \sum_{j\in\mathbb{Z},j\neq i} \frac{A_j - A_i}{d(j,i)^\mu} + \sum_{j\in\mathbb{Z},j\neq i} \frac{A_i}{d(j,i)^\mu} \\ &= \mathcal{L}A_i + 2l^{-\mu}A_i \sum_{k=1}^{\infty} \frac{1}{k^\mu} \\ &= \mathcal{L}A_i + 2l^{-\mu}A_i\zeta(\mu), \end{aligned} \tag{2.18}$$

where $\mathcal{L}$ is a functional defined by

$$\mathcal{L}f(i,t) = \sum_{j\in\mathbb{Z},j\neq i} \frac{f(j,t) - f(i,t)}{d(j,i)^\mu}.$$

We note here that the condition $\mu > 1$ makes $\zeta(\mu)$ finite. When l is small, we can make an approximation

$$\mathcal{L}f(i,t) = \sum_{j\in\mathbb{Z},j\neq i} \frac{f(j,t) - f(i,t)}{d(j,i)^\mu} \approx \frac{1}{l^d} \int_{y\in\mathbb{R}^d} \frac{f(y) - f(i)}{|y-i|^\mu} \mathrm{d}y,$$

where d is the dimension of the model, and the integral is interpreted as the principal value (to make it well-defined). Thus, we can approximate

$$\begin{aligned}\frac{1}{\sum_{j\in\mathbb{Z},j\neq i} w_{i\to j}} &= \frac{1}{2l^{-\mu}\zeta(\mu)A_i\left(\frac{\mathcal{L}A_i}{2l^{-\mu}\zeta(\mu)} + 1\right)} \\ &\approx \frac{1}{2l^{-\mu}\zeta(\mu)A_i} - \frac{\mathcal{L}A_i}{(2l^{-\mu}\zeta(\mu))^2}. \end{aligned} \tag{2.19}$$

Next, the equation for number of criminals is now

$$N(s,t+\delta t) = \sum_{i\in\mathbb{Z},i\neq s} N_i \cdot (1-p_i) \cdot q_{i\to s} + \Gamma\delta t, \tag{2.20}$$

as the criminals who have committed crimes at site i with probability $p_i = 1 - e^{-A_i\delta t}$ are removed. Let $z = 2\zeta(t)$. Subtracting $N(s,t)$ from both sides, dividing by δt, and taking limit $\delta t \to 0$, we get (note that N_t is now $\partial N/\partial t$)

$$\begin{aligned} N_t - \Gamma &\approx \lim_{\delta t\to 0} \frac{1}{\delta t}\left[-N_s + \sum_{i\in\mathbb{Z},i\neq s} N_i\cdot(1-A_i\delta)\frac{A_s}{|s-i|^\mu}\left(\frac{1}{A_i z} - \frac{l^\mu\mathcal{L}A_i}{(A_i z)^2}\right)\right] \\ &\approx \lim_{\delta t\to 0} \frac{A_s}{\delta t} \sum_{i\in\mathbb{Z},i\neq s}\left[\frac{\frac{N_i}{A_i} - \frac{N_s}{A_s}}{z d(s,i)^\mu} l^\mu - \frac{N_i}{|s-i|^\mu}\frac{l^\mu\mathcal{L}A_i}{A_i^2 z^2} - \frac{N_i}{|s-i|^\mu}\frac{l^\mu}{Dz}\right] \\ &= \frac{Dl^d}{z}\left(A\mathcal{L}\left(\frac{N}{A}\right) - A\sum_{i\in\mathbb{Z},i\neq s}\frac{N_i}{|s-i|^\mu}\frac{\mathcal{L}A_i}{A_i^2 z} - \frac{A}{z}\sum_{i\in\mathbb{Z},i\neq s}\frac{N_i}{|s-i|^\mu}\right) \end{aligned} \tag{2.21}$$

where $D = \frac{l^{\mu-d}}{\delta t}$. Using the same technique, we arrive at

$$N_t = \frac{D}{z}\left[A\Delta^*\left(\frac{N}{A}\right) - \frac{N}{A}\Delta^* A\right] - NA + \Gamma - l^\mu\left(\frac{AD}{z^2}\Delta^*\left(\frac{N\Delta^* A}{A^2}\right) + \frac{A}{z}\Delta^* N\right), \tag{2.22}$$

for which we have used

$$\Delta^* f(x,t) = \lim_{l\to 0} l^d \mathcal{L} f(x,t) = \int_{y\in\mathbb{R}^d} \frac{f(y)-f(x)}{|y-x|^\mu} dy.$$

Now we will try to connect this to the notations used in the fractional calculus. For ease of writing, let

$$s = \frac{\mu - d}{2}. \tag{2.23}$$

Recall the definition of the fractional Laplacian or Riesz Derivative (for example in [8])

$$-(-\Delta)^s f(x) = C_{d,2s}\int_{y\in\mathbb{R}^d} \frac{f(x)-f(y)}{|x-y|^{2s+d}} dy, \quad C_{d,2s} = 2^{2s}\frac{\Gamma(s+d/2)}{\pi^{d/2}|\Gamma(-s)|}, \quad 0 < s \le 1. \tag{2.24}$$

To see a connection to our Δ^*, we note that

$$\Delta^* = -C_{d,2s}^{-1}(-\Delta)^s.$$

For the remaining of this paper, for ease of writing, we abuse notation to write

$$-(-\Delta)^s \text{ as } \Delta^s. \tag{2.25}$$

We then instead define $D_2 = \frac{D}{C_{d,\mu-d}} = \frac{l^{2s}}{C_{d,2s}\delta t}$. Thus, the modified 1D model with a Lévy walk is

$$B_t = \frac{\eta D_1}{z_1} B_{xx} - \omega B + \varepsilon D_1 \rho A, \tag{2.26a}$$

$$N_t = \frac{D_2}{z_2}\left[A\Delta^s\left(\frac{N}{A}\right) - \frac{N}{A}\Delta^s A\right] - NA + \Gamma, \tag{2.26b}$$

where $D_1 = \frac{l^2}{\delta t}$, $D_2 = \frac{l^{2s}}{C_{d,2s}\delta t}$, $z_1 = 2$, and $z_2 = 2\zeta(\mu)$. Dividing (2.26b) by l^2 and using $\rho = N/l^2$ and $\gamma = \Gamma/l^2$ as in (2.14), we get

$$\rho_t = \frac{D_2}{z_2}\left[A\Delta^s\left(\frac{\rho}{A}\right) - \frac{\rho}{A}\Delta^s A\right] - \rho A + \gamma \tag{2.26b$'$}$$

One problem with this derivation is that it does not continuously move between the Lévy Flight and Brownian motion cases, since $C_s \to 0$ as $s \to 1$. This causes D_2 to diverge as we approach the traditional Laplacian. Some derivations avoid this problem by using different transition probabilities, see [1, 15]. However, these methods seem hard to fathom in the case of human mobility, as the probability distributions are more complicated and less natural. To avoid the divergence of D_2, we will simply let $D_2' = C_s D_2$. Hereafter the prime will be disregarded.

2.3. **Computer Simulation.**

2.3.1. *Discrete Model.* Using the discrete model, we implemented agent-based computer simulations in both one and two spatial dimensions. Our focus, however, will be on the 1-dimensional model, since the continuous simulations will also be in this dimension. Furthermore, the 2-dimensional simulation is an extension of the 1-dimensional case. The number of lattice points and the spacing between them, l, are self-assigned by the user. The boundary conditions of the model are periodic so that results can coincide with continuous simulations generated using spectral methods. We compiled a deterministic and stochastic version of the model.

For the deterministic version, we start with baseline attractiveness, A_0, and an initial criminal field of $\overline{N} + 0.01\cos(6\pi x)$, where, as in [13],

$$\overline{N} = \frac{\Gamma \delta t}{1 - e^{\overline{A}\delta t}}, \quad \overline{A} = A_0 + \overline{B}, \quad \overline{B} = \frac{\theta \Gamma}{\omega}. \tag{2.27}$$

The probability a crime will be committed at each lattice point is a function of the attractiveness, $p(s) = 1 - e^{-A_s(t)\delta(t)}$. We tabulate the number of crimes committed at each point by evaluating its expected value, $p(s)A(s)$, hence the deterministic nature of the model. The remaining criminals must move, and are assigned to the other positions on the grid by again evaluating the expected number of criminals to each point. The new criminal distribution and attractiveness are calculated in preparation for the next iteration. The stochastic model does not use expected values. The number of criminals are rounded to the nearest integer, allowing us to independently determine whether each criminal commits a crime, and where each will move if they don't commit a crime. To compensate for rounding, we add integer criminals with a probability determined by the criminal growth rate.

2.3.2. *Continuous Model: Pseudo-Spectral.* To simulate (2.26a) and (2.26b′), we used a pseudo-spectral method of lines with a stiff solver (MATLAB 23s or 15s). That is, we discretize in space but remain continuous in time. To calculate the fractional Laplacians, we use the fact that

$$\mathcal{F}_{x\mapsto q}\left\{\Delta^s f(x)\right\} = -|q|^{2s}\mathcal{F}_{x\mapsto q}\{f(x)\}. \tag{2.28}$$

Taking advantage of spectral accuracy allows us to use a small number of grid points. However, it also meant that we had to assume periodic boundary conditions. Still, there are considerable difficulties in implementing other boundary conditions.

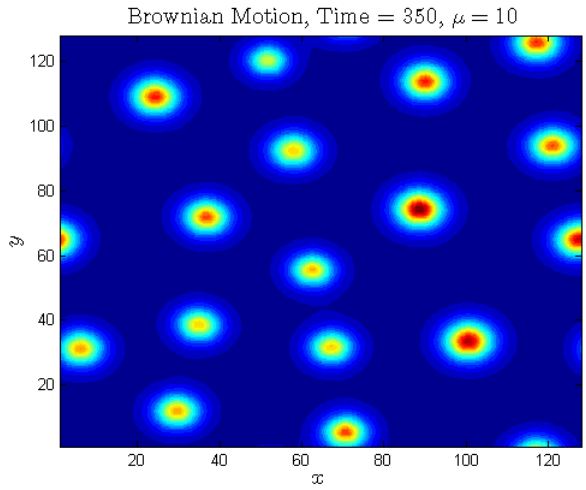

(a)

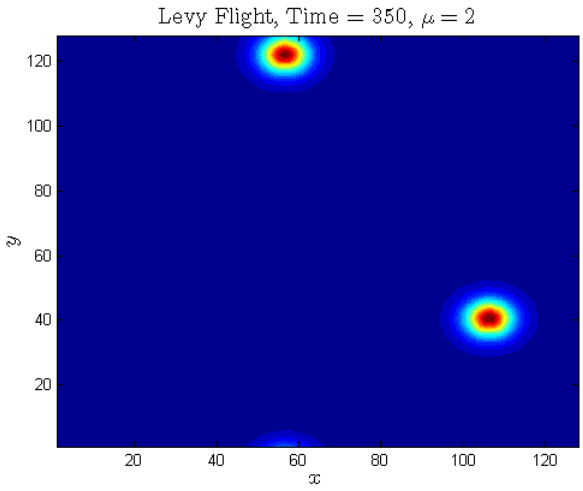

(b)

FIGURE 1. An agent-based simulation for the discrete model with criminals following Brownian Motion and Lévy flight.There is a heat map color coding, with red indicating high attractiveness and blue corresponding to low attractivenss. Fig 1(a): Simulation under Browniam motion conditions. The parameters are grid size = 128×128, time $= 350$, $\eta = 0.03$, $\theta = 0.56$, $\gamma = 0.019$, $\mu = 10$. Having $\mu = 10 > 3$ corresponds to Brownian Motion. Fig 1(b): The simulation under Lévy flight conditions. The parameters are the same as before, except $\mu = 2$. Because $\mu < 3$, the criminals follow Lévy flight. Also, the total attractiveness over the entire space is equal for the two simulations by the conservation property of this model. As a result, the Lévy flight peaks are larger because there are fewer hotspots.

3. Dispersion Relationship: Linear Stability Analysis

3.1. **Crime Model.** To non-dimensionalize, we set $\tilde{A} = A/\omega$, $\tilde{\rho} = (\varepsilon D_1/\omega)\,\rho$, $\tilde{x} = \sqrt{\frac{z_1\omega}{D_1}}x$, and $\tilde{t} = \omega t$. We further set[1] constants so that $\frac{D_2}{D_1}\cdot\frac{z_1}{z_2} = 1$. We substitute this into Eqs. (2.26) and drop the tildes to get

$$B_t = \eta B_{xx} - B + \rho A, \tag{3.1a}$$

$$\rho_t = \left(A\Delta^s\left(\frac{\rho}{A}\right) - \frac{\rho}{A}\Delta^s A\right) - \rho A + \overline{B}, \tag{3.1b}$$

where $\rho = N/l^2$, $\gamma = \Gamma/l^2$, $\overline{B} = \frac{\varepsilon D_1\gamma}{\omega^2}$. The spatially and temporally homogeneous solution does not change from before:

$$\overline{A} = A^0 + \overline{B} \quad \text{and} \quad \overline{\rho} = \frac{\overline{B}}{A^0 + \overline{B}}. \tag{3.2}$$

Then we look at the solutions of the form

$$A(x,t) = \overline{A} + \delta_A e^{\sigma t}e^{ik\cdot x}, \tag{3.3a}$$

$$\rho(x,t) = \overline{\rho} + \delta_\rho e^{\sigma t}e^{ik\cdot x}. \tag{3.3b}$$

This gives

$$\begin{bmatrix} -\eta|k|^2 - 1 + \overline{\rho} & \overline{A} \\ \frac{2\overline{\rho}}{\overline{A}}|k|^{2s+2} - \overline{\rho} & -|k|^{2s} - \overline{A} \end{bmatrix}\begin{bmatrix}\delta_A \\ \delta_\rho\end{bmatrix} = \sigma\begin{bmatrix}\delta_A \\ \delta_\rho\end{bmatrix}. \tag{3.4}$$

We note that any positive σ will lead to linear instability. Since the trace of the coefficient matrix in the Eq (3.4) is negative, a linear instability will occur at wavenumber k for which the determinant is negative, that is, when

$$\eta|k|^{2s+2} - |k|^{2s}(3\overline{\rho} - 1) + \eta\overline{A}|k|^2 + \overline{A} < 0. \tag{3.5}$$

Hence, there exists some parameter regime for which our system is unstable. A necessary condition for hotspots being formed from the homogeneous equilibrium is

$$\overline{\rho} > \frac{1}{3}, \tag{3.6}$$

or equivalently

$$\overline{B} > \frac{A^0}{2}. \tag{3.7}$$

3.2. **Cauchy process.** In order to better understand this stability result, we will investigate the situation when $s = 0.5$, The Eq. (3.5) becomes a cubic polynomial inequality

$$P(|k|) = \eta|k|^3 + \eta\overline{A}|k|^2 - |k|(3\overline{\rho} - 1) + \overline{A} < 0. \tag{3.8}$$

Note that $P(0) = \overline{A} > 0$. By Descartes' rule of signs, we can see that $P(x)$ has exactly one negative root, leaving two possibilities: (a) $P(x)$ has one negative root and two positives roots, or (b) $P(x)$ has one negative root and two complex roots. We can see that case (a) will give us a negative value of $P(x)$ in between two positive roots, if the two positive

[1]There are some issues here. If we let $f(s) = \frac{D_2}{D_1}\cdot\frac{z_1}{z_2} = \frac{l^{2s-2}}{\zeta(2s+1)C_{d,2s}}$, then we can see that $f(s)$ blows up as $s \to 1$. For the purpose of this paper, we will ignore this issue. See the end of §2.2 for more details.

roots are distinct. This regime corresponds to a linear instability. These two cases for polynomials $P(x) = ax^3 + bx^2 + cx + d$ can be distinguished by the discriminant

$$\Delta = 18abcd - 4b^3d + b^2c^2 - 4ac^3 - 27a^2d^2. \tag{3.9}$$

Case (a) with an additional condition that the two positive roots are distinct corresponds to $\Delta > 0$, while Case (b) corresponds to $\Delta < 0$. The inequality $\Delta > 0$ turns into

$$-4\overline{A}^4\eta^2 + \overline{A}^2\eta(9\overline{\rho}^2 - 60\overline{\rho} - 8) + 4(3\overline{\rho} - 1)^3 > 0. \tag{3.10}$$

This gives

$$8\eta\overline{A}^2 < 9\overline{\rho}^2 - 60\overline{\rho} - 8 + \sqrt{3\overline{\rho}(8 + 3\overline{\rho})^3}. \tag{3.11}$$

When $A^0 = 0$ (or $\overline{\rho} = 1$), the above expression becomes

$$\frac{\varepsilon^2\eta D^2}{\omega^2} \cdot \left(\frac{\gamma}{\omega}\right)^2 < \frac{-43 + 11\sqrt{33}}{8} \approx 2.52. \tag{3.12}$$

The physical interpretation of the above relationship is similar to that given in [13].

3.3. **A general case.** We prove the following result:

Result 1. *For $\overline{\rho} > \frac{1}{3}$, a condition for linear instability for the system Eq.* (3.4) *is*

$$\overline{A} < \overline{A}_*(\overline{\rho}, \eta, s) \equiv \left(\frac{-3\overline{\rho}(1-s) - 2s + \sqrt{W}}{2\eta s}\right)^s \left(\frac{3\overline{\rho}(1+s) - \sqrt{W}}{-3\overline{\rho}(1-s) + \sqrt{W}}\right), \tag{3.13}$$

where $W = 3\overline{\rho}(3\overline{\rho}(1-s)^2 + 4s)$. If $\overline{\rho} \le \frac{1}{3}$, then the system is stable.

Proof. From the condition given in Eq. (3.5), the system is unstable if and only if there is a value $|k|$ such that

$$\overline{A} < \frac{3\overline{\rho}|k|^{2s}}{1 + \eta|k|^2} - |k|^{2s}. \tag{3.14}$$

Let $g(|k|) = \frac{3\overline{\rho}|k|^{2s}}{1+\eta|k|^2} - |k|^{2s}$ and $\overline{A}_*(\overline{\rho}, \eta, s) = \sup_{|k|} \{g(|k|)\}$. Then, there is an instability when $\overline{A} < A_*$. Using Mathematica, we solved $\frac{d}{d|k|}g(|k|) = 0$. The equation turns out to be a quadratic equation in $|k|^2$, which has a unique non-negative solution, say $|k_0|$. We have $|k_0|^2 = \frac{-3\overline{\rho}(1-s) - 2s + \sqrt{W}}{2\eta s}$. We also checked that at $|k| = |k_0|$, $\frac{d^2}{d|k|^2}g(|k|) < 0$ to confirm that $|k_0|$ is in fact a maximum point. Finally, using Mathematica, we can simplify $g(|k_0|)$ to the right hand side of the equation Eq. (3.13), as desired. For $\overline{\rho} \le \frac{1}{3}$, it is clear that there is no $|k|$ satisfying Eq. (3.14). □

Remark. The condition given in Result 1 reduces to the condition given in Short *et al.* when $s = 1$, and it also reduces to our condition for the Cauchy process (Eq. (3.11)) when $s = \frac{1}{2}$. See § 3.4.1 for the numerical test of Result 1, and the results agree favorably.

We can prove a similar result for $\overline{\rho}$. Suppose $|k_*|$ is the unique root of $|k|^{2s+2} + \overline{A}(1 - s)|k|^2 - \frac{\overline{A}s}{\eta} = 0$. Then the condition for instability is equivalent to

$$\overline{\rho} > \overline{\rho}_*(\overline{A}, \eta, s) \equiv \frac{1}{3}\left(1 + \eta|k_*|^2\right)\left(1 + \frac{\overline{A}}{|k_*|^{2s}}\right). \tag{3.15}$$

We can see that we cannot get a solution in closed form when solving for $\overline{\rho}$, but we deduce that there is a $\overline{\rho}_*(\overline{A}, \eta, s)$ for which the system is unstable if and only if $\overline{\rho} > \overline{\rho}_*$.

3.4. **Theory Versus Numerics.**

3.4.1. *Set-up.* The larger eigenvalue of Eq. (3.4) is

$$\sigma(|k|) = \frac{1}{2}\left(-J + \sqrt{J^2 - 4(\overline{A} + |k|^{2s})(1 + \eta|k|^2) + 12|k|^{2s}\overline{\rho}}\right), \tag{3.16}$$

where $J = 1 + \overline{A} + \eta|k|^2 + |k|^{2s} - \overline{\rho}$.

Using Mathematica to solve $\frac{\partial \sigma}{\partial s} = 0$, we find that there are two points of k, say k_1 and k_2, such that $\mathrm{Re}(\sigma(k))$ is independent of s. And the values are given by

$$|k_1| = 1, \quad |k_2| = \sqrt{\frac{6(\overline{\rho} - \frac{1}{3}) + 3\overline{A}}{2\eta}}. \tag{3.17}$$

3.4.2. *Hot-Spot Detection.* We need to automate a hot-spot detection to distinguish between hot-spot and no-hot-spot outcomes (see Fig. 4, for example).

The following is a list of methods that we use to detect hot-spots.

- The variance and its derivative.
- The difference of the maximum of the solution in the final frame from $\overline{A}$ as a percentage of $\overline{A}$.
- The difference between the maximum and the minimum.
- An ensemble method (a combination of the above methods).

3.4.3. *Results.* See Figure 6 for the numerical test of Result 1. For most cases, the results agree favorably. There are some false negatives (detection of hotspot where we did not predict) near the bifurcation curve. In some cases, especially when $\overline{A}$ is small, there are substantial. This could be due to the numerical solver or hot-spot detection. It also may reflect that for some parameters values we have oscillating hotspots, see Figure 5, which our hotspot detection methods are not equiped to address.

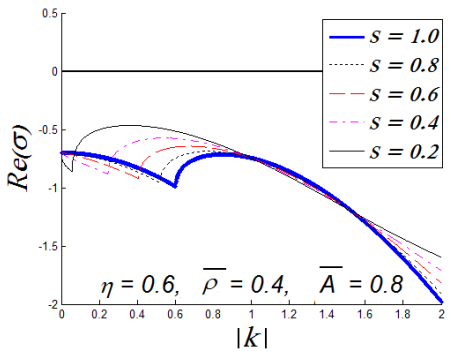

(a) A stable regime

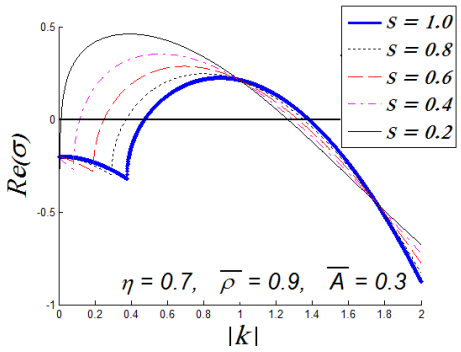

(b) An unstable regime

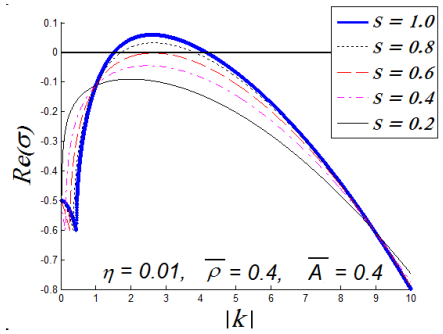

(c) Fractional diffusion leads to stability

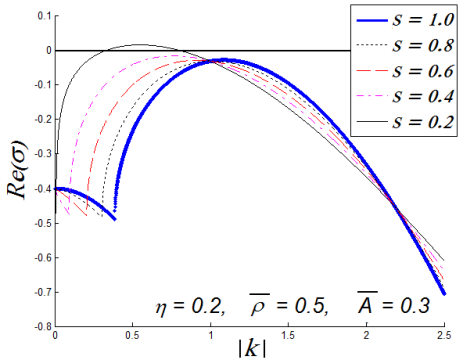

(d) Fractional diffusion leads to unstability

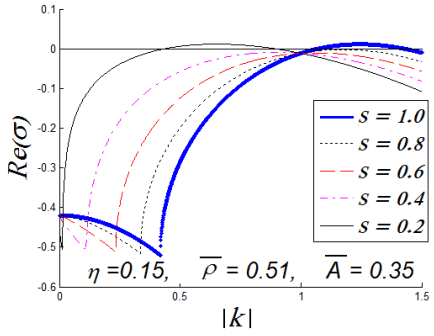

(e) Fractional diffusion leads to stability and then instability

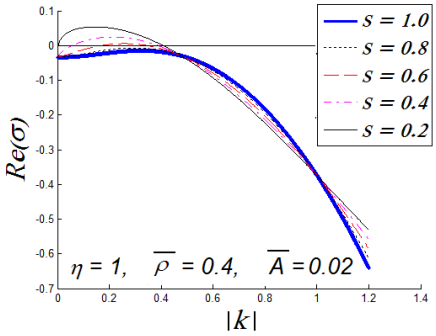

(f) A regime in which $|k_2| < |k_1| = 1$

FIGURE 2. Different possibilities of the effect of fractional diffusion based on Eq. (3.16)

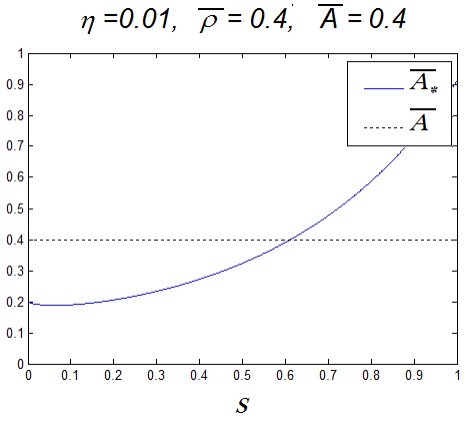

(a) Fractional diffusion leads to stability

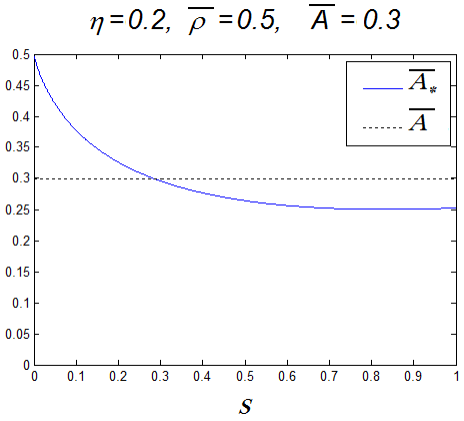

(b) Fractional diffusion leads to unstability

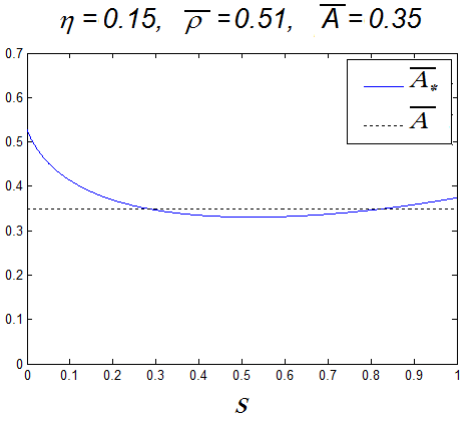

(c) Fractional diffusion leads to stability and then instability

FIGURE 3. Different possibilities of the effect of fractional diffusion based on Eq. (3.13). Note that Fig. 3(a) corresponds to Fig. 2(c); Fig. 3(b) corresponds to Fig. 2(d); and Fig. 3(c) corresponds to Fig. 2(e);

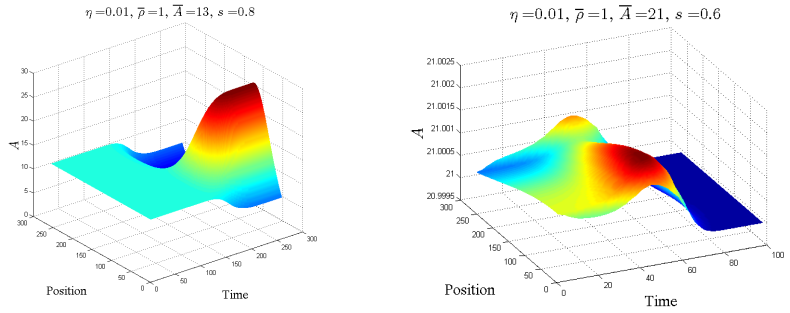

(a) A hot-spot formation when $\overline{A} = 13$, $s = 0.8$.

(b) No hot-spot formation when $\overline{A} = 21$, $s = 0.6$.

FIGURE 4. Possible outcomes of the system.

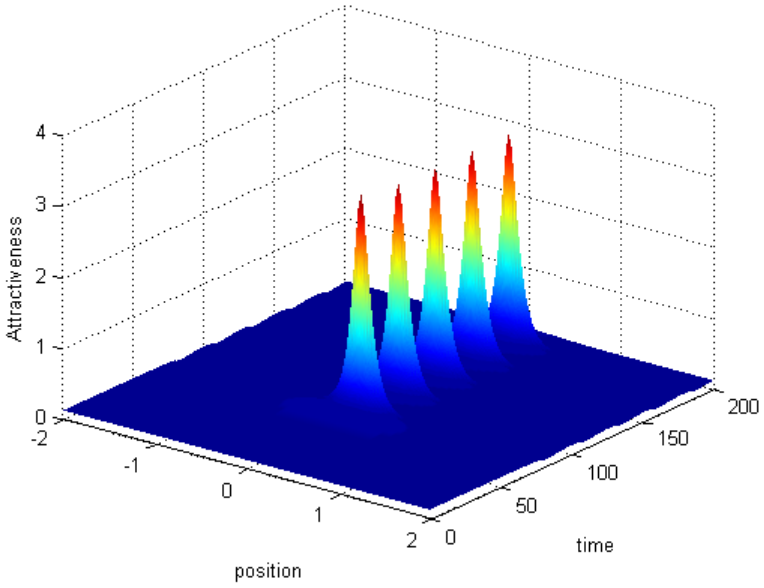

FIGURE 5. A hotspot solution that oscillates in time

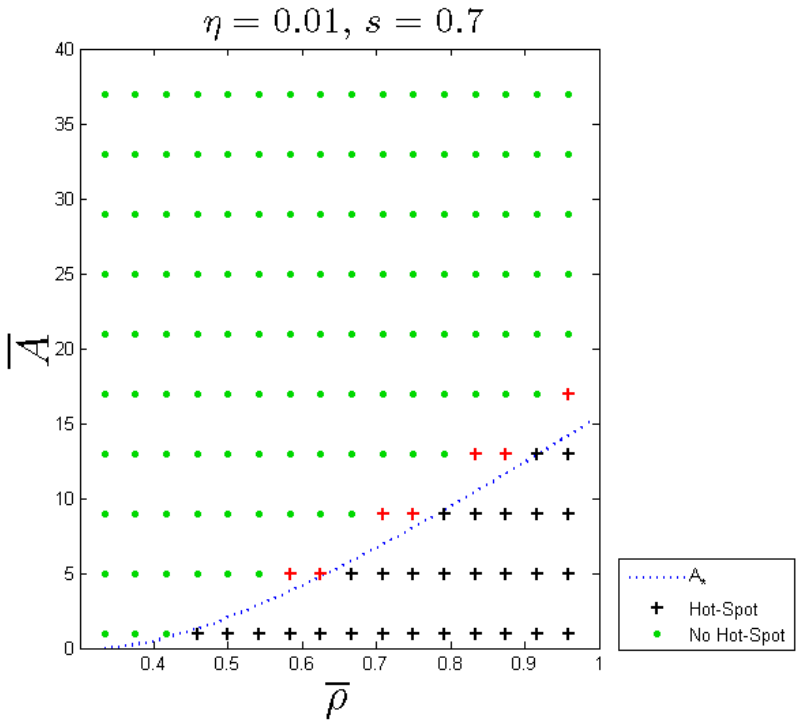

(a) A cross section in which only $\overline{\rho}$ and $\overline{A}$ vary.

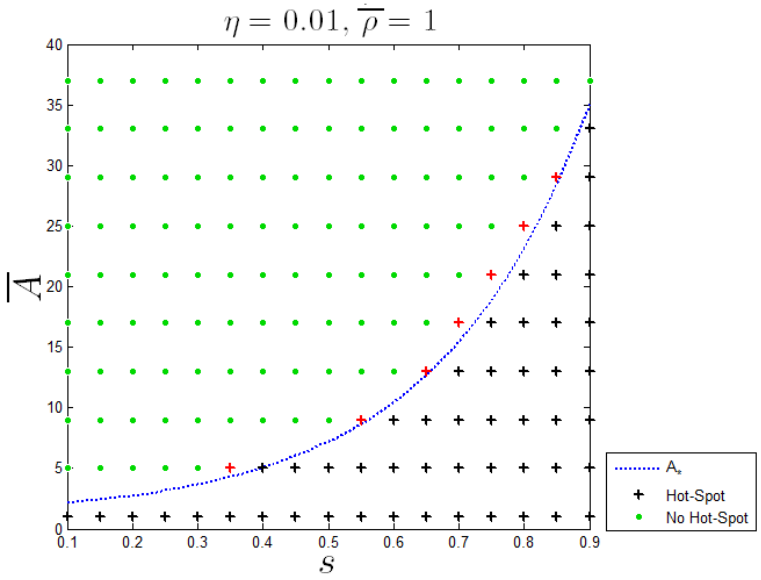

(b) A cross section in which only s and $\overline{A}$ vary.

FIGURE 6. Numerically testing Result 1. Red pluses denote the error of detecting hot-spots where we did not predict. From the diagram, this error happens only near the blue bifurcation curve.

4. HOT-SPOTS

4.1. **Profile.**

4.1.1. *Asymptotic Analysis of Steady-State Hot-Spot Solutions in 1-D for Lévy Flight Model.* Motivated by the technique that works for the Brownian walking criminal model in [5], we investigate the shape or profile of a stable hotspot in the interval $[-L, L]$. First, we introduce a new variable V,

$$V = \frac{\rho}{A^2}. \tag{4.1}$$

Then,

$$A\Delta^s\left(\frac{\rho}{A}\right) - \frac{\rho}{A}\Delta^s A = A\Delta^s(VA) - VA\Delta^s A. \tag{4.2}$$

Notice that, if we hold V constant, the above term is zero, which will be important in the analysis of the shape of the hot-spots. Eqs. (3.1) become

$$B_t = \eta B_{xx} - B + VA^3, \tag{4.3a}$$

$$(VA^2)_t = A\Delta^s(VA) - VA\Delta^s A - vA^3 + \overline{B}. \tag{4.3b}$$

Notably, for any functions P and Q, the integration of $P\Delta^s Q - Q\Delta^s P$ is zero, since

$$\begin{aligned}\int_{-\infty}^{\infty} P\Delta^s Q - Q\Delta^s P dx &= \int_{-\infty}^{\infty}\int_{-\infty}^{\infty} \frac{P(x)Q(y) - P(y)Q(x)}{|x-y|^{2s+1}} dy dx \\ &= 0,\end{aligned} \tag{4.4}$$

by symmetry. This also means that the fractional Laplacian operator is self-adjoint under the inner product

$$\langle p, q\rangle = \int_{-\infty}^{\infty} p(x)q(x)dx. \tag{4.5}$$

Note that this result also holds if we replace the infinite limits with $[-L, L]$. Thus, integrating the steady-state of Eq. (4.3b), we get

$$V = \frac{2L\overline{B}}{\int_{-L}^{L} A^3 dx}. \tag{4.6}$$

Now we proceed following the analysis of Kolokolnikov *et al* [5] . We begin by changing the variables as follows (together with $\hat{A} = \tilde{A}, \hat{\rho} = \tilde{\rho}$): $\hat{\varepsilon}^2 = \eta, \hat{\alpha} = A_0, \hat{x} = \sqrt{\hat{D}}\tilde{x}, \hat{t} = \hat{\tau}\tilde{t},$ and $\hat{\gamma} = \hat{\alpha} + \frac{\varepsilon D\gamma}{\omega}$, where $A_0 = A - B = \hat{A} - \hat{B}$. After dropping the hats, we have

$$A_t = \varepsilon^2 A_{xx} - A + VA^3 + \alpha, \tag{4.7a}$$

$$\tau(VA^2)_t = D\left(A\Delta^s(VA) - VA\Delta^s A\right) - VA^3 + \gamma - \alpha, \tag{4.7b}$$

and note that $\alpha < \gamma$. Let $y = x/\varepsilon$. Then, Eq. (4.7a) becomes $B_t = B_{yy} - B + VA^3$. By an analogy to Kolokolnikov *et al*. [5], for $D \gg \varepsilon^2$, we get $V = O(\varepsilon^2)$ globally on $-L < x < L$, $A = O(\varepsilon^{-1})$ in the inner region, $A = O(1)$ in the outer region, $D = O(\varepsilon^{-2})$, and $P = O(1)$ in the inner region. This analysis leads to a change of variables

$$V = \varepsilon^2 v, \quad D = \frac{D_0}{\varepsilon^2}, \tag{4.8}$$

where we have both v and D_0 of order $O(1)$, leading to

$$\begin{aligned} A_t &= \varepsilon^2 A_{xx} - A + \varepsilon^2 v A^3 + \alpha, && \text{(4.9a)} \\ \tau\varepsilon^2 (vA^2)_t &= D_0 \left(A\Delta^s(vA) - vA\Delta^s A\right) - \varepsilon^2 v A^3 + \gamma - \alpha. && \text{(4.9b)} \end{aligned}$$

4.1.2. *A Single Steady-State Hot-Spot Solution.* By the result in the previous section, it makes sense to expand

$$A = \frac{A_0}{\varepsilon} + A_1 + \cdots, \quad v = v_0 + \varepsilon v_1 + \cdots, \quad y = \frac{x}{\varepsilon}. \tag{4.10}$$

Note that by change of variables, we have

$$\Delta^s u(x) = \varepsilon^{2s} \Delta^s U(y), \tag{4.11}$$

where $U(y) = u(x) = u(\varepsilon y)$. In what follows, we will write U as u for convenience. Thus, $u(x)$ and $u(y)$ will actually represent the same thing, depending on the context. In terms of y, from Eq (4.9a), we get

$$\begin{aligned} (A_0)_{yy} - A_0 + v_0 A_0^3 &= 0, \quad -\infty < y < \infty, && \text{(4.12a)} \\ (A_1)_{yy} - A_1 + 3A_0^2 A_1 v_0 &= -\alpha - v_1 A_0^3, \quad -\infty < y < \infty. && \text{(4.12b)} \end{aligned}$$

In terms of x, let $\mathcal{L}^s(g(x), h(x)) = g\Delta^s h - h\Delta^s g$, for any valid functions g and h. Note that when $s = 1$, we have $\mathcal{L}^1(g, hg) = (g^2 h')'$. From Eq (4.9b), we get, in terms of y,

$$\begin{aligned} \mathcal{L}^s(A_0, v_0 A_0) &= 0, && \text{(4.13a)} \\ \mathcal{L}^s(A_0, v_1 A_0) + \mathcal{L}^s(A_0, v_0 A_1) + \mathcal{L}^s(A_1, v_0 A_0) &= 0, && \text{(4.13b)} \end{aligned}$$

where $-\infty < y < \infty$.

Lemma 1. *If, for all x,*

$$\Delta^s(v_0 A_0) = v_0 \Delta^s A_0, \tag{4.14}$$

then v_0 must be constant.

Proof. Suppose for contrary that there are x_1, x_2 such that $v(x_1) \neq v(x_2)$. Without loss of generality, suppose $v(x_1) > v(x_2)$. By definition, we have

$$\begin{aligned} 0 &= \left(\Delta^s(v_0 A_0) - v_0 \Delta^s A_0\right)_{x=x_2} - \left(\Delta^s(v_0 A_0) - v_0 \Delta^s A_0\right)_{x=x_1} \\ &= c \int_{-\infty}^{\infty} \frac{A(y)(v(x_1) - v(x_2))}{|x - y|^{\mu}} dy \\ &> 0, \end{aligned}$$

a clear contradiction. □

By Lemma 1, from Eqs. (4.13a) and (4.13b), we deduce that v_0 and v_1 must be constants.

Using the same trick as in Kolokolnikov *et al.* [5], from Eq. (4.12a), we can write the homoclinic solution with the condition $(A_0)_y(0) = 0$ as

$$A_0(y) = v_0^{-1/2} w(y), \tag{4.15}$$

where w is the unique solution to the ground-state problem

$$w'' - w + w^3 = 0, \quad -\infty < y < \infty; \quad w(0) > 0, w'(0) = 0; \quad w \to 0 \text{ as } |y| \to \infty, \tag{4.16}$$

which is given explicitly by

$$w = \sqrt{2}\operatorname{sech} y. \tag{4.17}$$

Similarly to arguments in §2.1 in Kolokolnikov *et al.* [5], we get the same hot-spot shape for the attractiveness field A but a different shape of v in the second order. The detailed results are as follows:

Result 2. *In the inner region ($|x| < \varepsilon$),*

$$A(y) \sim \varepsilon^{-1} A_0(y) + A_1(y) + \cdots, \tag{4.18}$$

$$A_0(y) = v_0^{-1/2} w(y), \tag{4.19}$$

$$A_1(y) = \alpha(1 - [w(y)]^2) - \frac{v_1}{2v_0^{3/2}} w(y), \tag{4.20}$$

where v_0 and v_1 are unknown constants, and $w(y) = \sqrt{2}\operatorname{sech} y$.
In the outer region ($\varepsilon \ll |x| \le l$), from Eqs. (4.9)*, we have*

$$A = \alpha + o(1) \tag{4.21a}$$

$$v = h_0(x) + o(1). \tag{4.21b}$$

Substituting in Eq. (4.9b)*, we get*

$$\Delta^s h_0(x) = \zeta = \frac{\alpha - \gamma}{D_0 \alpha^2} < 0, \quad 0 < |x| \le l, \quad (h_0)_x(\pm l) = 0, \tag{4.22}$$

subject to the matching condition that $h_0(x) \to v_0$ as $x \to 0^{\pm}$.

We now embark on a brief digression, because the estimate for v does correspond with the numerical result, in contrast to the estimate for A. This is an area of continuing investigation. The following are some fractional differential equations we have worked on that may help us improve our estimate for v.

Lemma 2. *The solution to $\Delta^s u = \delta(x)$ on $(-\infty, \infty)$ is, up to a shift by constant,*

$$u(x) = u_{del} \equiv c_1 |x|^{2s-1}, \tag{4.23}$$

where $c_1 = \frac{\Gamma(2(1-s))\sin(s\pi)}{(2s-1)\pi}$, for $\frac{1}{2} < s < 1$; and $c_1 = \frac{1}{2}$, for $s = 1$. Also,

$$u'(\pm L) = (2s-1) c L^{2s-2}. \tag{4.24}$$

Proof. We first consider the case when $s = 1$. Via Fourier transform, we get

$$2\pi u(x) = -\operatorname{Re}\int_{-\infty}^{\infty} \frac{e^{ikx}}{|k|^2}dk = -\operatorname{Re}\int_{-\infty}^{\infty} \frac{e^{ikx}}{k^2}dk. \tag{4.25}$$

We take the derivative to get

$$2\pi u'(x) = \int_{-\infty}^{\infty} \frac{\sin(kx)}{k}dk = \operatorname{sgn}(x)\int_{-\infty}^{\infty} \frac{\sin(y)}{y}dy = \operatorname{sgn}(x)\pi, \tag{4.26}$$

where we change the variables $y = kx$. Thus, $u(x) = \frac{1}{2}|x| + \text{const}$.
For $s < 1$, we have

$$\begin{aligned} 2\pi u(x) &= -\operatorname{Re}\int_{-\infty}^{\infty} \frac{e^{ikx}}{|k|^{2s}}dk \\ &= -2\int_0^{\infty} \frac{\cos(kx)}{k^{2s}}dk. \end{aligned} \tag{4.27}$$

Again, we take the derivative to get

$$2\pi u'(x) = 2\int_0^{\infty} \frac{\sin(kx)}{k^{2s-1}}dk \tag{4.28}$$

$$= 2\Gamma(2(1-s))\sin(s\pi)\operatorname{sgn}(x)\frac{(x^2)^s}{x^2}, \quad \frac{1}{2} < s < 1. \tag{4.29}$$

Thus, we get

$$\begin{aligned} u(x) &= \frac{\Gamma(2(1-s))\sin(s\pi)}{(2s-1)\pi}(x^2)^{s-\frac{1}{2}} + \text{const} \\ &= \frac{\Gamma(2(1-s))\sin(s\pi)}{(2s-1)\pi}|x|^{2s-1} + \text{const}, \end{aligned} \tag{4.30}$$

and we note that

$$\lim_{s\to 1^-} \frac{\Gamma(2(1-s))\sin(s\pi)}{(2s-1)\pi} = \frac{1}{2}, \tag{4.31}$$

which corresponds to the classical Laplacian case. □

Lemma 3. *The solution to the equation $\Delta^s u = rect\left(\frac{x}{2L}\right)$ on the interval $(-\infty, \infty)$ is, up to a shift by constant,*

$$u(x) = u_{rect} \equiv c_2\left[((L+x)^2)^s sgn\,(L+x) + ((L-x)^2)^s sgn\,(L-x)\right], \tag{4.32}$$

where $c_2 = \frac{\Gamma(-2s)\sin(s\pi)}{\pi}$. Note that, for $s > \frac{1}{2}$, we have

$$\lim_{x\to\pm L} u'(x) = c_2\left(2s(2L)^{2s-1}\right). \tag{4.33}$$

Proof. We use Mathematica to calculate in the Fourier space to get the above result. □

Now we are ready to solve the following problem.

Problem Statement. Solve

$$\Delta^s u = \text{rect}\left(\frac{x}{2L}\right) + c_0\delta(x). \tag{4.34}$$

The problem is to choose c_0 such that $u'(\pm L) = 0$. In that case, what is $u(x)$?

Solution. The solution is $u = u_{del} + c_0 u_{rect}$, for $s > \frac{1}{2}$. By solving $u'(\pm L) = 0$, we get $c_0 = \frac{2^{2s-1}L}{1-2s}$.

□

4.2. **Gierer-Meinhardt System.** Considering our difficulties with the crime model, we decided to investigate a different model that exhibits pattern formation, the Gierer-Meinhardt model, in the hopes that a fractional version of it might provide some insight into the system presented above. The Gierer-Meinhardt system is given by

$$A_t = \varepsilon^2 A_{xx} - A + \frac{A^2}{H}, \tag{4.35a}$$

$$0 = H_{xx} - H + A^2. \tag{4.35b}$$

First, we perform the asymptotic analysis on the traditional GM model. Later, we replace H_{xx} with $\Delta^s H$ and analyze the dynamics of the system.

In the inner region, let $x = \varepsilon y$, where ε is small. This gives $H \sim H_0$. If we let $A = H_0 w$, then $w_{yy} - w + w^2 = 0$ has an explicit solution of $w = \frac{3}{2}\text{sech}^2(y/2)$.

In the outer region, we have $H_{yy} - H \sim 0$, which has the explicit solution $H = \frac{1}{\varepsilon \int_0^\infty w^2 dy} e^{-|x|}$.

After some asymptotic analysis, we get equilibrium solutions as follows: (letting $y = x/\varepsilon$)

$$A_e = H_0 w(y), \tag{4.36a}$$

$$H_e = H_0 e^{-|x|}, \tag{4.36b}$$

$$H_0 = \frac{1}{\varepsilon \int_0^\infty w^2 dy}. \tag{4.36c}$$

4.2.1. *Steady-State Stability.* We perturb the equilibrium solutions as usual to get

$$\lambda\varphi = \varepsilon^2 \varphi_{xx} - \varphi + \frac{2A}{H}\varphi - \frac{A^2}{H^2}\psi \tag{4.37a}$$

$$0 = \psi_{xx} - \psi + 2A\varphi. \tag{4.37b}$$

In the outer region, this gives

$$\psi \sim \psi(0) e^{-x}, \tag{4.38}$$

and after integrating Eq. (4.37a), we get

$$\psi_0 = \frac{2\int_0^\infty w\varphi dy}{\int_0^\infty w^2 dy} \tag{4.39}$$

Thus, Eq. (4.37a) turns into

$$\lambda\varphi = \varepsilon^2 \varphi_{xx} - \varphi + 2w\varphi - \chi\left(\int_0^\infty w\varphi dy\right) w^2, \tag{4.40}$$

where $\chi = \frac{2}{\int_0^\infty w^2 dy}$. There is a theorem stating that Eq. (4.40) is stable, i.e. $\text{Re}(\lambda) \leq 0$ (see references in [5]), if and only if $\chi > \frac{1}{\int_0^\infty w^2 dy}$. This inequality holds for our case, meaning that the GM system is always stable near hot-spots.

4.2.2. *Fractional Diffusive GM System.* In the case of fractional diffusion term $\Delta^s H = \mathcal{D}_{|x|}^{2s} H$ replacing H_{xx}, we would expect Eq. (4.40) to be the same except $\chi = \chi^*$ for some new value χ^*. We can see that, in the inner region, $H \sim H_0$ and $A = H_0 w$, where w is the same as before. In the outer region, however, we need to solve $\Delta^s H - H \sim 0$.

In particular, we need $H(0^+)$. We can in fact explicitly compute this value. Suppose $A^2 \approx \left(\varepsilon \int_{-\infty}^{\infty} A^2 dy\right) \delta(x)$ in the inner region. If we let $H(x) = -\left(\varepsilon \int_{-\infty}^{\infty} A^2 dy\right) G(x)$, from $\Delta^s H - H + A^2 = 0$, we have

$$\Delta^s G - G = \delta(x), \tag{4.41}$$

and $H(0) = -\left(\varepsilon \int_{-\infty}^{\infty} A^2 dy\right) G(0)$. Since $A = H_0 w$ in the inner region, we get

$$H_0 = -\frac{1}{G_0 \varepsilon \int_{-\infty}^{\infty} w^2 dy}. \tag{4.42}$$

The upshot is

$$G_0 \equiv G(0) = \int_{-\infty}^{\infty} \frac{1}{1+|q|^{2s}} dq = \frac{2\pi \csc\left(\frac{\pi}{2s}\right)}{2s}, \quad 2s > 1. \tag{4.43}$$

In the inner region, we approximate $2A\varphi = \left(\varepsilon \int_{-\infty}^{\infty} 2A\varphi dy\right) \delta(x)$. From $\Delta^s \psi - \psi + 2A\varphi = 0$, we get

$$\psi = -\left(\varepsilon \int_{-\infty}^{\infty} 2A\varphi dy\right) G. \tag{4.44}$$

It turns out that, in the inner region, because $\Delta^s \psi - \psi \sim 0$,

$$\psi \sim \psi(0) = -2\varepsilon H_0 G_0 \int_{-\infty}^{\infty} w\varphi dy = \frac{2}{\int_{-\infty}^{\infty} w^2 dy} \int_{-\infty}^{\infty} w\varphi dy, \tag{4.45}$$

which does not depend on the value of G_0. So, $\chi = \frac{2}{\int_{-\infty}^{\infty} w^2 dy}$. Thus, we conclude that we always have stable hotspots.

5. DISCUSSION

Simple, seemingly minor changes in assumptions about human mobility resulted in major differences in the dynamics. Moreover, introducing Lévy Flight to the model created many difficulties. From the standpoint of finding numerical solutions, part of the system becomes fully non-linear. Further, the linear stability result becomes far more complicated, introducing bifurcations in the Lévy Flight non-locality parameter s. Additional work is needed to ensure that the hotspot detection is truly working and distinguish the false positives and true negatives. While the shape of the hotspots in the attractiveness field does not change under the non-local model, it seems likely that the hotspots in ρ assume a different shape. Further research will investigate the presence of a Hopf Bifurcation, weakly non-linear stability, perturbation near hotspots, stability of single and arbitrary numbers of hotspots, and the dynamics of the model after the addition of police.

6. ACKNOWLEDGMENTS

We would like to thank our mentors Profs. Theodore Kolokolnikov and Scott McCalla for being very helpful and supportive. Thanks also to UCLA for this researching opportunity and Harvey Mudd College Mathematics Department for funding Tum Chaturapruek. Finally, thanks Nestor Guillen for creating the Nonlocal Equations Wiki (`http://www.ma.utexas.edu/mediawiki`).

REFERENCES

[1] Rudolf Gorenflo, Gianni De Fabritiis, and Francesco Mainardi. Discrete random walk models for symmetric lévyfeller diffusion processes. *Physica A: Statistical Mechanics and its Applications*, 269(1):79 – 89, 1999.

[2] Barry D. Hughes, Michael F. Shlesinger, and Elliott W. Montroll. Random walks with self-similar clusters. *Proceedings of the National Academy of Sciences*, 78(6):3287–3291, 1981.

[3] Alex James, Michael J. Plank, and Andrew M. Edwards. Assessing lvy walks as models of animal foraging. *Journal of The Royal Society Interface*, 8(62):1233–1247, 2011.

[4] P. Jeffery Chayes Lincoln R. Jones, Paul A. Brantingham. Statistical models of criminal behavior: The effects of law enforcement actions. *Mathematical Models and Methods in Applied Sciences*, 20:1397 – 1423, 2010.

[5] T. Kolokolnikov, M. Ward, and J. Wei. The Stability of Steady-State Hot-Spot Patterns for a Reaction-Diffusion Model of Urban Crime. *ArXiv e-prints*, January 2012.

[6] A.L. Schwartz I.B. Marthaler, D Bertozzi. Levy searches based on a priori information: The biased levy walk. *UCLA CAM Report*, 4(50), 2004.

[7] Ralf Metzler and Joseph Klafter. The random walk's guide to anomalous diffusion: a fractional dynamics approach. *Physics Reports*, 339(1):1 – 77, 2000.

[8] Y. Nec. Spike-type solutions to one dimensional gierermeinhardt model with lvy flights. *Studies in Applied Mathematics*, pages no–no, 2012.

[9] Ashley B. Pitcher. Adding police to a mathematical model of burglary. *European Journal of Applied Mathematics*, 21(Special Double Issue 4-5):401–419, 2010.

[10] Injong Rhee, Minsu Shin, Seongik Hong, Kyunghan Lee, Seong Joon Kim, and Song Chong. On the levy-walk nature of human mobility. *IEEE/ACM Trans. Netw.*, 19(3):630–643, June 2011.

[11] M. Short, M. D Orsogna, P. Brantingham, and G. Tita. Measuring and modeling repeat and near-repeat burglary effects. *Journal of Quantitative Criminology*, 25:325–339, 2009. 10.1007/s10940-009-9068-8.

[12] M. B. Short, P. J. Brantingham, and M. R. D'Orsogna. Cooperation and punishment in an adversarial game: How defectors pave the way to a peaceful society. *Phys. Rev. E*, 82:066114, Dec 2010.

[13] M. R. Pasour V. B. Tita G. E. Brantingham P. J. Bertozzi A. L. Chayes L. B. Short, M. B. D'Orsogna. A statistical model of criminal behavior. *Mathematical Models and Methods in Applied Sciences*, 18:1249 – 1267, 2008.

[14] M.B. Short, P.J. Brantingham, A.L. Bertozzi, and G.E. Tita. Dissipation and displacement of hotspots in reaction-diffusion models of crime. *Proceedings of the National Academy of Sciences of the United States of America*, 107:3961–3965, 2010.

[15] A. Zoia, A. Rosso, and M. Kardar. Fractional laplacian in bounded domains. *Phys. Rev. E*, 76:021116, Aug 2007.